Society of Medical Education & Research

2022, Volume 2, Issue 1, Page No: 85-98
ISSN: 3108-4826

Journal of Medical Sciences and Interdisciplinary Research

The HBV S Gene C138R Mutation Induces Occult Infection through Defective HBsAg Antigenicity and Secretion

Mohamed Ibrahim Hassan[1]*, Ahmed Youssef Nabil[1]

[1]Department of Business Administration, Faculty of Commerce, Cairo University, Cairo, Egypt.

***E-mail** ✉ m.hassan.cu@gmail.com

Abstract

Occult hepatitis B virus infection (OBI) is associated with substantial risks of transmission and disease progression. Alterations in the S gene are regarded as key factors in the emergence of OBI. A prior investigation by our group detected the C138R substitution in the S gene among individuals with OBI. The present work sought to examine the influence of the C138R substitution on HBsAg functionality and the underlying processes responsible for OBI. Complete HBV genome constructs (HBV 1.3, genotype B) and corresponding mutant constructs (HBV C138R) were generated, together with HA-tagged expression vectors for wild-type (sWT) and mutant (sC138R) S proteins. The consequences of the C138R substitution on HBsAg antigenicity, secretion, and dimerization were assessed via transfection experiments in cultured cells and hydrodynamic tail vein delivery in mice. The C138R substitution dramatically lowered both intracellular and extracellular HBsAg concentrations while leaving HBV transcription, replication, and expression of other viral proteins unaffected. Experiments using HA tagging showed that the decline stemmed from reduced antigenicity. Data from multiple commercial ELISA assays and HA detection in culture media indicated that the C138R substitution additionally hindered HBsAg secretion. The C107R substitution likewise substantially diminished both antigenicity and secretion of HBsAg. Non-reducing Western blot analysis combined with AlphaFold 3 structural modeling demonstrated that the C138R substitution promoted the assembly of atypical HBsAg dimers. These observations were corroborated in the murine HBV model.The C138R substitution promotes OBI by concurrently compromising HBsAg antigenicity and secretion. The main mechanism involves breakage of the disulfide bridge between residues 107 and 138, leading to the generation of conformationally aberrant dimers that impair HBsAg function.

Keywords: Occult hepatitis B virus infection, S gene variants, HBsAg antigenicity, HBsAg secretion, Disulfide bond, HBsAg dimer

Introduction

Recent progress in diagnostic virology has improved the precise detection and treatment of cases classically defined by HBsAg positivity. Nevertheless, identifying and handling occult hepatitis B virus infection (OBI) continues to pose difficulties and represents a significant barrier to meeting the World Health Organization's target of eradicating viral hepatitis as a public health concern by 2030 [1, 2]. OBI is characterized by undetectable HBsAg despite the existence of replication-capable HBV DNA in liver tissue and/or serum [3]. Due to its subtle presentation, OBI frequently evades standard testing. Critically, OBI is not a harmless carrier condition; it retains transmissibility and can progress to HBV reactivation under immunosuppression or other stimuli, potentially contributing to hepatocellular carcinoma [4, 5]. OBI also creates substantial risks in vulnerable populations, blood product safety, organ donation, and the choice of therapeutic regimens [6, 7]. Thus, OBI remains a critical challenge for efficient HBV screening and control.

Access this article online https://smerpub.com/

Received: 27 November 2021; **Accepted:** 19 February 2022

How to cite this article: Hassan MI, Nabil AY. The HBV S Gene C138R Mutation Induces Occult Infection through Defective HBsAg Antigenicity and Secretion. J Med Sci Interdiscip Res. 2022;2(1):85-98. https://doi.org/10.51847/aBB6TXFeEH

The HBV genome contains four overlapping open reading frames: preC/C, P, X, and preS/S [8]. The preS/S frame produces the large (LHBs), middle (MHBs), and small (SHBs) envelope polypeptides from separate initiation sites; these are collectively designated HBsAg [9]. SHBs, the predominant form, comprises 226 amino acids and features a major hydrophilic region (MHR), four transmembrane segments, and two cytoplasmic loops [10]. The segment from amino acids 124 to 147 inside the MHR, termed the ‘a’ determinant, harbors key epitopes recognized by neutralizing antibodies and constitutes the principal antigenic cluster across HBV genotypes [11]. Variants in the ‘a’ determinant are strongly linked to OBI, including the classic G145R change and others such as G130R, M133T, and N146S [2, 12]. These changes can evade HBsAg detection by modifying antigenicity, immune recognition, or export efficiency [13], and may further impair virion replication or release [14, 15]. Together, such effects drive the establishment and maintenance of OBI.

Earlier work from our laboratory revealed numerous S gene alterations in OBI cases, including a cysteine-to-arginine change at residue 138 (C138R) situated within the “a” determinant. As far back as 2003, this identical C138R variant was found in a patient with pre-existing anti-HBs who progressed to chronic hepatitis and cirrhosis [16]. Later reports verified its occurrence in OBI. For instance, a 2024 analysis showed that, across 24 residues in the “a” determinant, position 138 had the fifth-highest mutation rate, with all changes being C138R [17]. A study in Mexico also detected this variant in S gene sequences from HIV-positive individuals with OBI [18]. To clarify the contribution of C138R to OBI pathogenesis, we developed two plasmid systems: (1) a wild-type full-length HBV construct (HBV 1.3, genotype B) and its C138R mutant (HBV C138R); and (2) HA-tagged wild-type (sWT) and mutant (sC138R) S protein expression vectors. By employing cell transfection in vitro and hydrodynamic injection in mice in vivo, we comprehensively analyzed the impact and mechanisms of the C138R substitution on HBsAg biological properties, offering new mechanistic understanding and diagnostic perspectives for OBI.

Materials and Methods

Construction of various plasmids

The HBV C138R mutant construct was created using the 1.3-mer full-length HBV genome plasmid (pGEM-HBV1.3B, subtype adw2; GenBank accession number AY220698.1), which includes nucleotides 1038–3215 and 1–1984 of the HBV genome. The HBV C138R variant was produced by replacing cysteine with arginine at amino acid position 138 in the original HBV 1.3 plasmid. Utilizing the HBV genome sequence (nucleotides 160–841), the S gene was chemically synthesized and inserted into the pXF3H vector to generate the sWT plasmid. Corresponding mutant constructs (sC138R, sC107R, sC124R, and sC147R) were developed by incorporating individual point mutations into the sWT plasmid. All wild-type and mutant HBsAg proteins expressed from these plasmids carried an N-terminal double HA tag (sequence: MYPYDVPDYANSPYPYDVPDYA). An empty vector served as a negative control.

Cell culture and transfection

Huh7, HepG2, and HEK293T cells were maintained in Dulbecco’s Modified Eagle Medium (DMEM; Gibco, USA) containing 10% heat-inactivated fetal bovine serum (FBS; Gibco, USA) and 1% penicillin-streptomycin. Cultures were kept at 37 °C in a 5% CO_2 humidified atmosphere. For transfection, 1.5 µg of plasmid DNA was combined with 3 µL of Lipofectamine 3000 (Invitrogen, USA, L3000-015) in 125 µL of Opti-MEM (Gibco, USA, 31985070) and allowed to stand for 15 min at room temperature. This complex was then applied to cells in 250 µL of Opti-MEM. Following 6 h incubation at 37 °C with 5% CO_2, the medium was exchanged for fresh complete DMEM. Cells were cultured for an additional 48 h under identical conditions prior to further experiments.

Quantification of various viral proteins

Culture supernatants were harvested by centrifugation 48 h post-transfection. Levels of HBsAg and HBeAg in supernatants and cell lysates were determined using the Abbott ARCHITECT i2000SR automated immunoassay platform. Non-reducing and reducing Western blotting were conducted to assess HBsAg and HA-tagged protein expression employing an anti-HBs antibody (Bioss, China, bs-1557G) and an anti-HA tag antibody (CST, USA, C29F4), as outlined previously [19]. HBcAg detection utilized an anti-HBcAg antibody (Abcam, UK, ab8637). GAPDH (Huabio, China, ET1601-4) served as the loading control. Furthermore, intracellular and extracellular HBsAg concentrations were evaluated with four different commercial ELISA kits following the manufacturers' instructions. The kits (1–4) were supplied by InTec PRODUCTS, INC. (Xiamen), Beijing Wantai Biological Pharmacy Enterprise Co., Ltd., Shanghai Rongsheng Biotech Co., Ltd., and Shanghai Kehua Bio-Engineering Co., Ltd., respectively.

Quantification of intracellular RNA by fluorescence quantitative PCR

SYBR Premix Ex Taq (Vazyme, China, Q311) was employed for fluorescence quantitative PCR to measure intracellular RNA abundance. Relative gene expression was calculated via the $2^{-\Delta\Delta Ct}$ method using Bio-Rad CFX Maestro software (Bio-Rad, USA). Human β-actin functioned as the housekeeping gene.

Quantification of HBV DNA by fluorescence quantitative PCR

HBV DNA in culture supernatants was isolated using a commercial hepatitis B virus nucleic acid extraction kit (Shengxiang, China). Real-time fluorescence PCR was then performed for quantification, with DNA levels derived from a standard curve prepared according to the kit protocol.

Immunofluorescence (IF) staining

Intracellular HBsAg and HA immunofluorescence staining, along with fluorescence intensity quantification, were carried out as reported earlier [20]. In brief, cells were grown on glass coverslips and transfected with the specified plasmids. At the designated time, cells were fixed in 4% paraformaldehyde, permeabilized with 0.25% Triton X-100, and blocked using 1% bovine serum albumin (BSA). Overnight incubation at 4 °C was performed with either anti-HBs or anti-HA tag primary antibodies. Following washes, cells were exposed for 1 h at room temperature to FITC-conjugated donkey anti-goat secondary antibody (green; Proteintech, China, SA00003-1) or Cy3-conjugated goat anti-rabbit secondary antibody (red; Proteintech, China, SA00009-1). Nuclei were stained with DAPI. Images were obtained with a ZEISS upright fluorescence microscope, ensuring uniform acquisition settings across samples.

Construction of HBV model in mice

Male BALB/c mice aged 6–8 weeks were maintained in specific pathogen-free (SPF) facilities. All experimental procedures complied with institutional animal welfare standards and were approved by the Animal Ethics Committee of Anhui Medical University (No. LLSC2012004). To establish the HBV model, 10 µg of HBV 1.3 plasmid was dissolved in physiological saline at a volume corresponding to 0.1 mL per gram of body weight and rapidly injected (within 10 s) into the tail vein of each mouse. The HBV C138R and blank control (BK) models were similarly produced by injecting the HBV C138R plasmid or empty vector, respectively. Each experimental group initially comprised 15 animals.

Serological testing and liver immunohistochemical detection in mice Blood serum was gathered from every animal at intervals of days 1, 3, 5, 7, 10, 14, and 21 after model induction. At the points of days 3, 7, and 21, a subset of five animals from each cohort underwent euthanasia to procure hepatic specimens. Prior to termination on those specific days, venous blood was withdrawn from individual subjects. As a result, serum volumes were secured from 15 subjects per cohort during days 1 and 3, from 10 during days 5 and 7, and from 5 during days 10, 14, and 21. Hepatic extracts were obtained from five subjects per cohort across the three key timestamps (days 3, 7, and 21). Serum dilutions were set at 1:10 for evaluation of HBsAg and anti-HBs titers via the Abbott ARCHITECT i2000SR immunoassay apparatus. Hepatic sections were immobilized in 4% paraformaldehyde solution, paraffin-infiltrated, sliced, and stained immunohistochemically for HBsAg presence utilizing anti-HBs reagents.

Analysis of structural characteristics of SHBs dimers Structural modeling of wild-type and C138R-altered SHBs dimers was executed with AlphaFold 3 to identify and contrast conformational discrepancies. Visualization of these wild-type and C138R-altered dimer configurations was handled by the PyMOL application.

Statistical analysis Processing of datasets occurred through GraphPad Prism 8.0 (San Diego, CA, USA), with presentation in the format of averages ± SD. Cellular assays featured $n \geq 3$ instances per category across three separate runs. Data distribution normality was checked using the Shapiro-Wilk methodology. Pairwise contrasts for Gaussian-distributed sets applied two-sided unpaired t-testing; skewed distributions used Mann-Whitney assessments. Group variances among several sets were examined via one-way ANOVA incorporating Bonferroni adjustments for pairwise follow-ups. Markers of relevance included $P < 0.05$, $P < 0.01$, $P < 0.001$.

Results and Discussion

C138R mutation reduced intra- and extracellular HBsAg levels

For probing the C138R alteration's role in HBsAg synthesis, a standard HBV 1.3 vector and its paired C138R derivative were assembled**.** Vector authenticity and refinement were validated through gel electrophoresis on agarose**.** Independent transfections of Huh7 lines with HBV 1.3 or HBV C138R vectors were followed by HBsAg quantification employing chemiluminescent detection, immunofluorescence microscopy, and immunoblotting. Outcomes demonstrated pronounced drops in both cellular and media-based HBsAg for the C138R vector group versus the HBV 1.3 counterpart **(Figures 1a and c).** Equivalent patterns emerged in HepG2 and HEK293T transfectants under identical vector applications **(Figures 1d and e).**

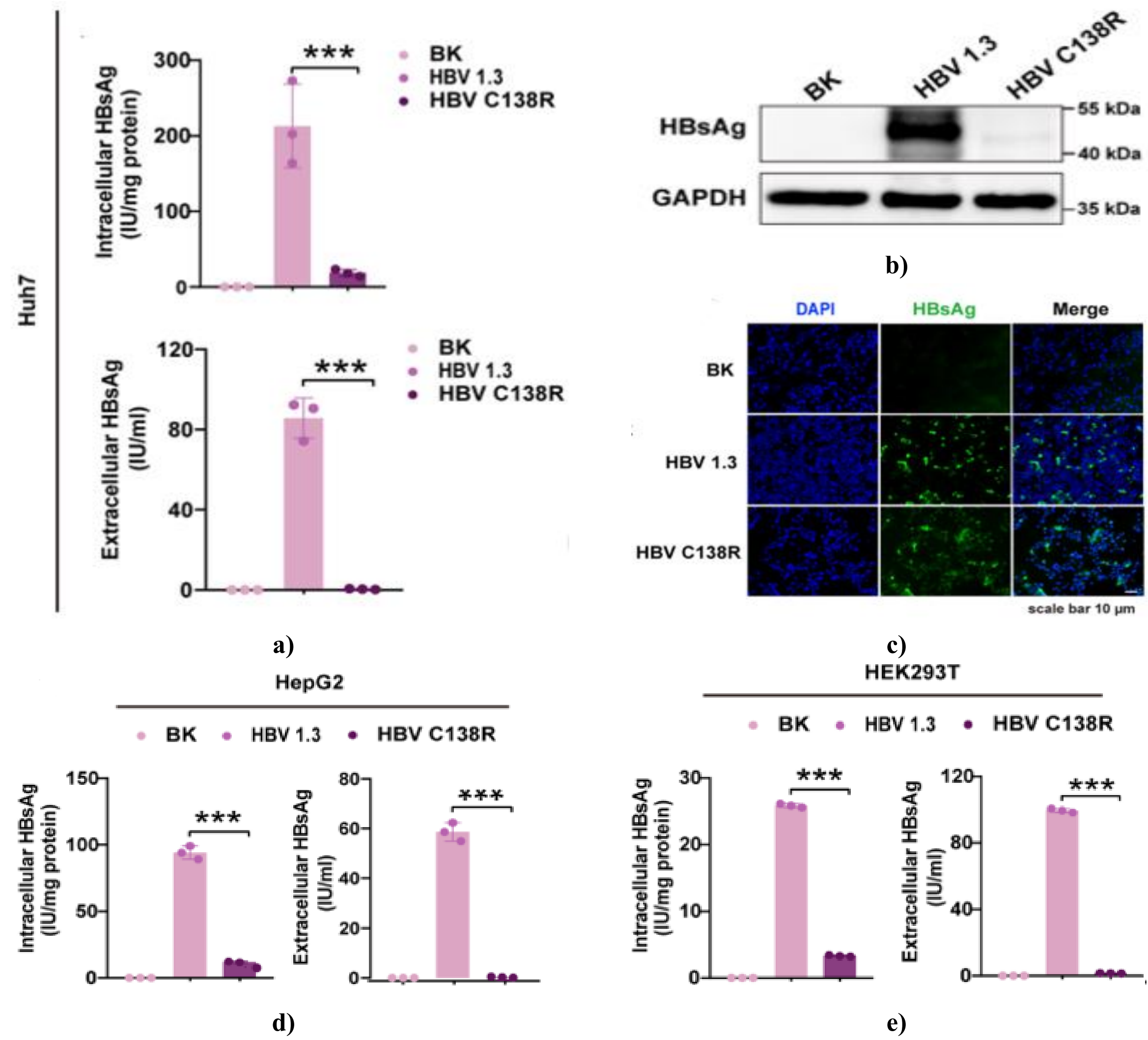

Figure 1. The S gene's 'α' determinant C138R variant decreased HBsAg quantities. (a) Cellular and secreted HBsAg from Huh7 transfectants with HBV 1.3 or HBV C138R vectors was assessed by Abbott luminescence detection. (b) Immunoblotting under non-reducing conditions captured HBsAg in Huh7 transfectants with HBV 1.3 or HBV C138R vectors. (c) Fluorescence microscopy examined HBsAg production and positioning in Huh7 transfectants with HBV 1.3 or HBV C138R vectors. (d-e) Cellular and secreted HBsAg quantification in HepG2 (d) and HEK293T (e) transfectants with HBV 1.3 or HBV C138R vectors via Abbott luminescence. Triplicate executions; averages ± SD. $P < 0.001$

C138R mutation did not affect HBV transcription, replication, or expression of other viral proteins

To evaluate broader viral impacts from the C138R change, Huh7 transfections occurred with either HBV 1.3 or HBV C138R vectors. No appreciable shifts arose in HBsAg mRNA content or in overall HBV transcripts and pgRNA quantities **(Figure 2a).** Secreted HBV DNA amounts likewise showed no distinctions across cohorts **(Figure 2b).** Additionally, HBeAg and HBcAg abundances aligned between the vector types **(Figures 2c and 2d)**. In summary, the C138R alteration uniquely curtailed HBsAg presence, sparing HBV gene activation, genome multiplication, and non-HBsAg protein synthesis.

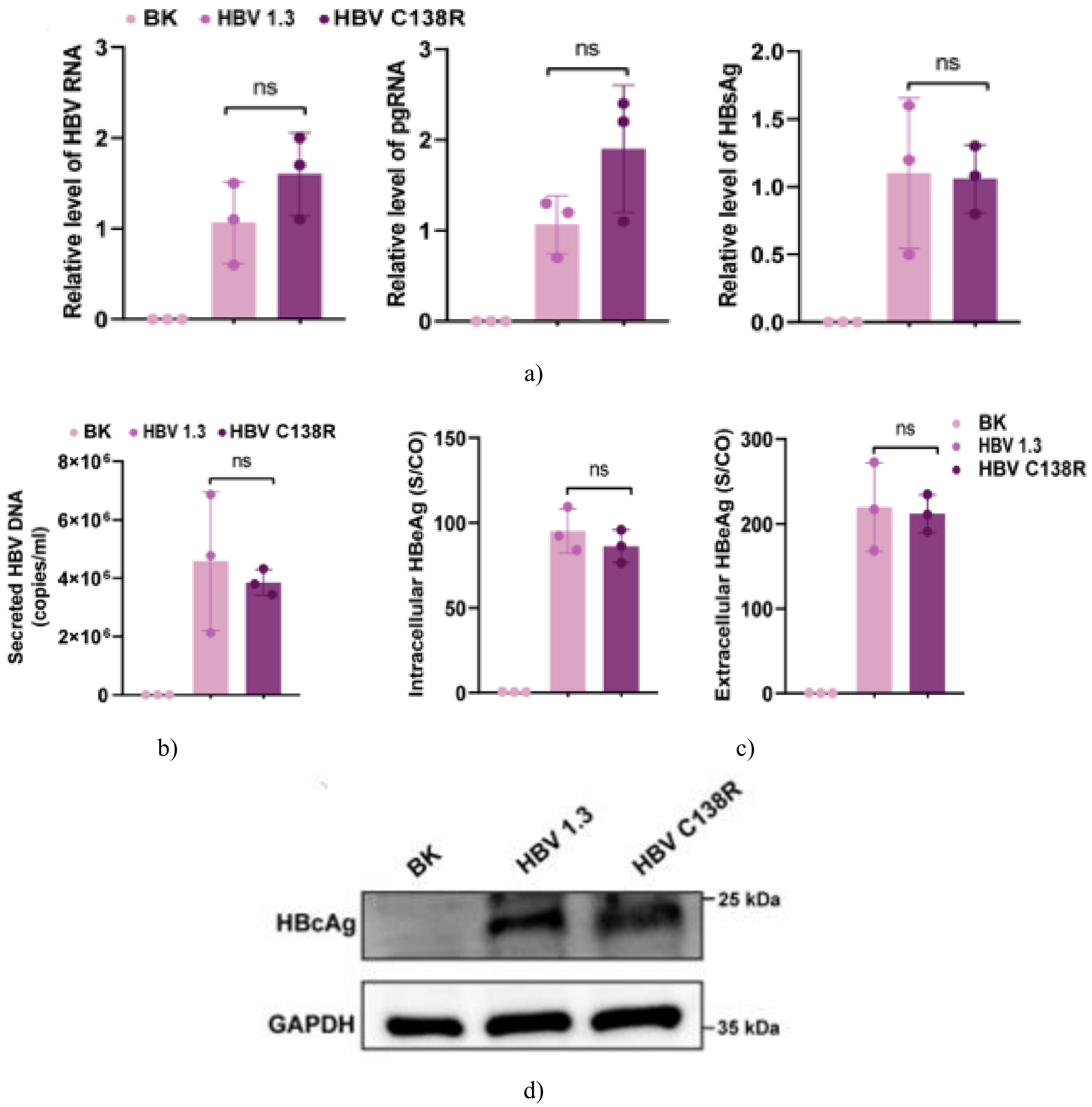

Figure 2. The C138R variant exerted no influence on HBV gene activation, genome amplification, or production of alternative viral components. (a) Normalized transcript quantities for total HBV RNA, pgRNA, and HBsAg mRNA in Huh7 transfectants harboring HBV 1.3 or HBV C138R vectors. (b) Extracellular HBV DNA concentrations in media from Huh7 cultures transfected with HBV 1.3 or HBV C138R vectors. (c) Cellular and secreted HBeAg quantities in Huh7 transfectants with HBV 1.3 or HBV C138R vectors, assessed via Abbott luminescent detection. (d) HBcAg protein detection by immunoblotting in Huh7 transfectants with HBV 1.3 or HBV C138R vectors. Triplicate determinations; values shown as average ± SD. pgRNA: pregenomic RNA;

HBsAg: hepatitis B surface antigen; HBeAg: hepatitis B e antigen; HBcAg: hepatitis B core antigen; ns: not significant

C138R mutation reduced HBsAg antigenicity

Considering the pivotal function of the ‘α’ determinant in HBsAg epitope exposure [19], HA-fused wild-type (sWT) and variant (sC138R) expression vectors were generated**.** Plasmid validation through gel separation confirmed proper assembly and purity. Following introduction into Huh7 lines, HBsAg quantification in cellular extracts and media revealed substantial declines for the sC138R variant relative to sWT **(Figures 3a-c).** Parallel declines appeared in HepG2 and HEK293T transfectants **(Figures 3e-f).** To distinguish between altered recognition versus synthesis, HA tag abundance was monitored inside and outside cells. Remarkably, internal HA signals in sC138R transfectants remained unchanged or slightly elevated compared to sWT **(Figures 3b and 3d).** This pattern indicated that the C138R change compromised HBsAg epitope recognition while leaving overall protein synthesis intact.

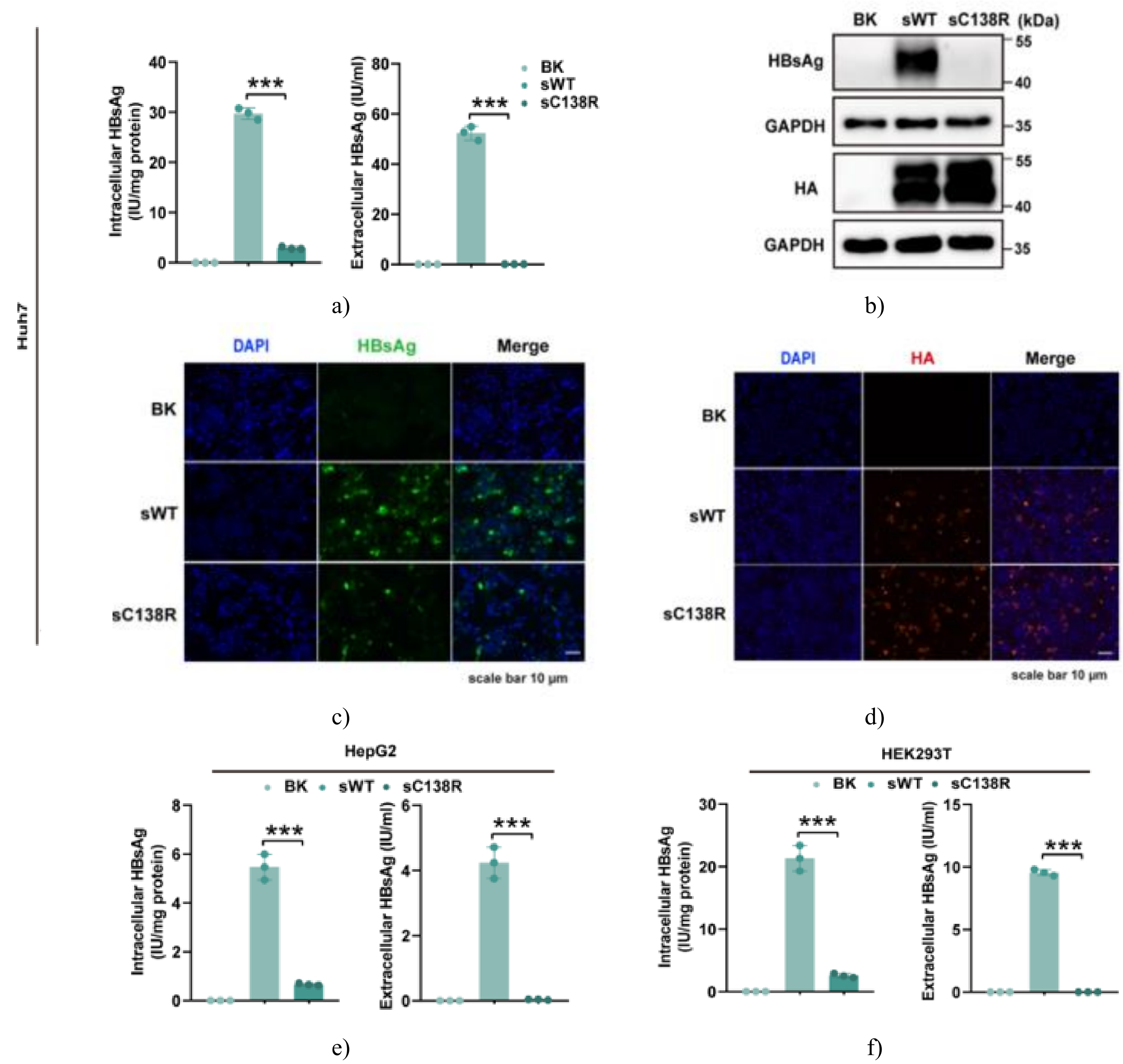

Figure 3. The C138R alteration diminished HBsAg epitope detection. (A) Cellular and secreted HBsAg from Huh7 transfectants with sWT or sC138R vectors, quantified by Abbott luminescence platform. (B)

Immunoblotting under non-reducing conditions for HBsAg and HA in Huh7 transfectants with sWT or sC138R vectors. (C-D) Fluorescence microscopy evaluation of HBsAg (C) and HA (D) distribution and abundance in Huh7 transfectants with sWT or sC138R vectors. (E-F) Cellular and secreted HBsAg quantification in HepG2 (E) and HEK293T (F) transfectants with sWT or sC138R vectors via Abbott luminescence. Triplicate assessments; averages ± SD. P < 0.001. HBsAg: hepatitis B surface antigen; HA: hemagglutinin; WB: western blotting; IF: Immunofluorescence

Multiple commercial ELISA kits confirmed that the C138R mutation markedly reduced both the antigenicity and secretion of HBsAg

For additional verification, four independent diagnostic ELISA platforms were applied to measure HBsAg inside and outside cells. Uniformly, both compartments displayed sharply lower signals in C138R-containing transfectants versus wild-type controls. Reactivity proved weakest against kit 1, approaching background levels, while kits 2, 3, and 4 retained minimal but measurable binding. In HBV C138R samples, residual detection with kits 2–4 spanned 6.28% to 30.35% of HBV 1.3 values. Correspondingly, sC138R-derived HBsAg retained 3.17% to 25.08% reactivity versus sWT **(Figures 4a-b).** Secretion ratios (extracellular/intracellular) for HBV C138R reached only 23.90%, 25.08%, and 28.13% of HBV 1.3 levels across kits 2–4. For sC138R, these ratios dropped to 23.58%, 13.22%, and 47.90% of sWT **(Figures 4c-d).** Supporting this, internal HA accumulation trended upward in sC138R cultures, yet extracellular HA signals were prominent in sWT media but virtually absent in sC138R **(Figure 4e).** Overall, the evidence established that the C138R variant profoundly disrupted both epitope accessibility and export of HBsAg.

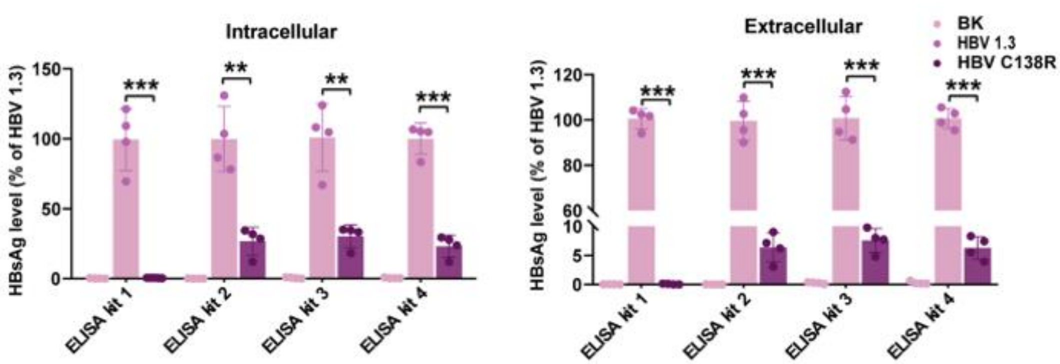

a)

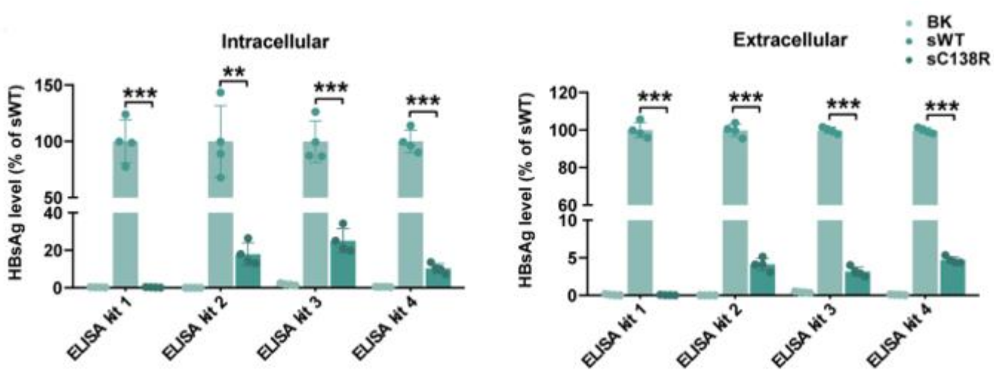

b)

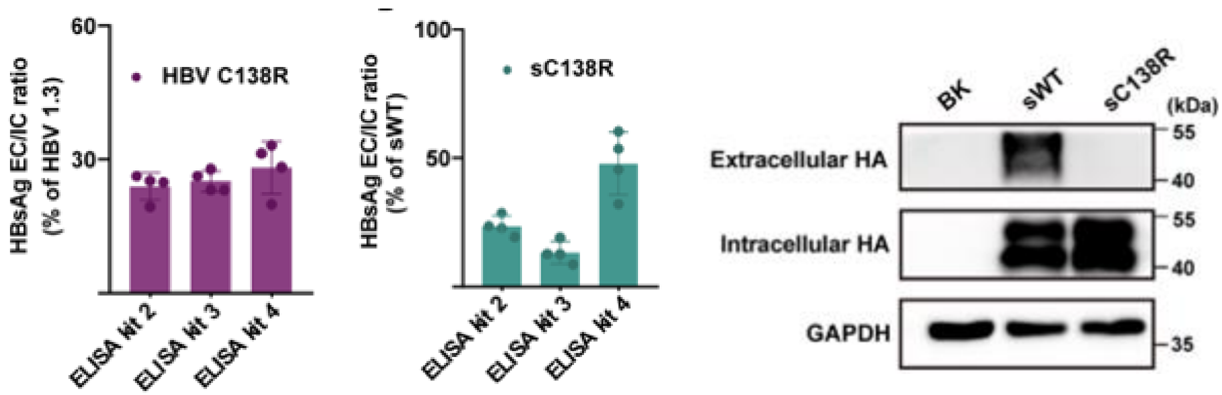

c) d) e)

Figure 4. Diverse diagnostic ELISA platforms verified that the C138R variant substantially compromised both epitope recognition and export of HBsAg. (a-b) Four independent ELISA systems assessed cellular and secreted HBsAg quantities in Huh7 cultures harboring complete HBV genomic vectors (a) or HA-fused S protein expression constructs (b). (c-d) Export-to-internal ratios (EC/IC) for HBsAg, normalized to wild-type cohorts, in Huh7 transfectants with HBV C138R vectors (c) or sC138R vectors (d). (e) Cellular and secreted HA protein detection in Huh7 transfectants with sWT or sC138R vectors via non-reducing immunoblotting. Triplicate measurements; averages ± SD shown. $P < 0.01$, $P < 0.001$. ELISA: enzyme-linked immunosorbent assay; HBsAg: hepatitis B surface antigen; EC/IC: extracellular-to-intracellular ratio; HA: hemagglutinin; WB: western blotting

Disruption of the disulfide bond between aa107 and aa138 reduced HBsAg antigenicity and secretion, as well as the formation of aberrant conformational dimers

The C138R alteration abolished the cysteine bridge linking residues 107 and 138. To explore how breakage of this bridge drives functional defects in HBsAg, a complementary sC107R construct was engineered to target the identical linkage. Additional variants, sC124R and sC147R, were created to interrupt alternative key bridges in the MHR domain. Each construct was delivered separately into Huh7 lines. Quantification revealed sharp declines in both internal and external HBsAg for C107R and C138R variants versus wild-type, moderate reduction with C124R, and negligible impact from C147R **(Figure 5a).** Internal HA abundance remained comparable across all variants. Secreted HA signals appeared clearly in C124R and C147R media but vanished almost entirely in C107R and C138R samples. Prior assays employed non-reducing conditions to maintain native multimeric states. To probe whether aberrant multimer assembly underlies the defects, reducing immunoblotting was applied. Non-reducing blots displayed prominent ~40 kDa dimeric HBsAg primarily in wild-type, with near-absent signals in C138R and related variants **(Figures. 1b, 3b and 5b).** Reducing conditions yielded equivalent ~20 kDa monomeric bands across all cohorts **(Figure 5c).** Parallel patterns emerged for HA: non-reducing conditions showed ~40 kDa species **(Figures. 3b, 4e and 5d),** while reducing conditions revealed ~20 kDa forms **(Figure 5e).** No notable HA expression variance occurred between wild-type and variants under either condition, implying formation of atypical dimers that evade detection. AlphaFold 3 modeling highlighted marked structural divergence between wild-type and C138R SHBs dimers (RMSD: 4.064) **(Figures 5f and s5).**

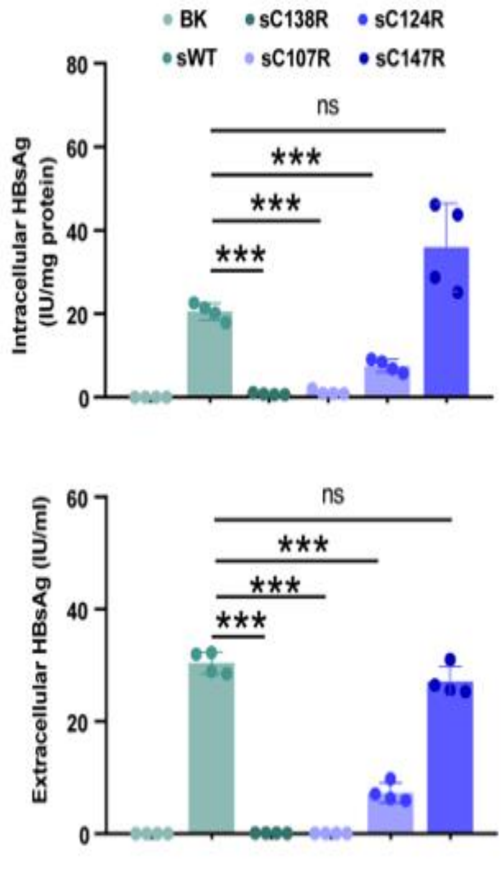

a)

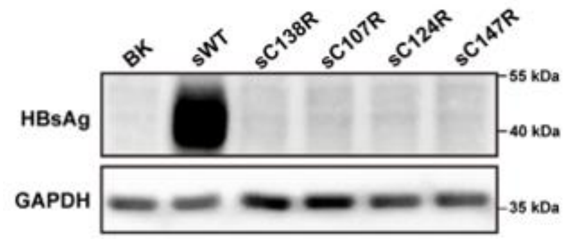

b)

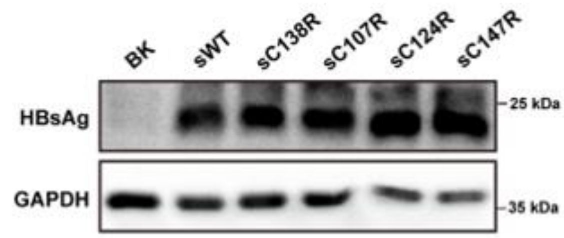

c)

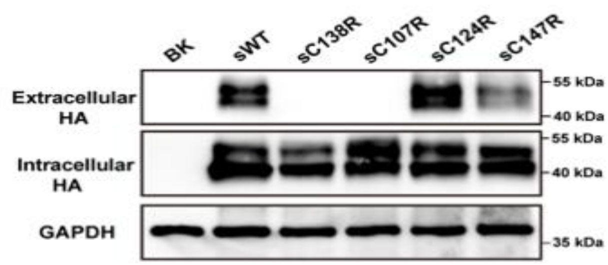

d)

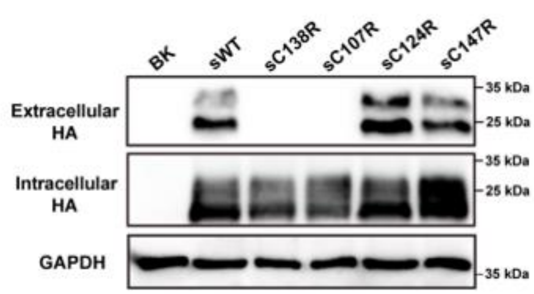

e)

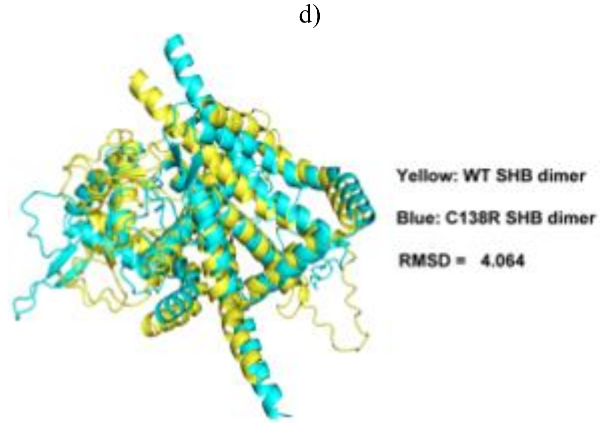

f)

Figure 5. Consequences of breaking distinct cysteine bridges within the 'α' determinant on HBsAg epitope exposure, export, and dimer assembly. (a) Cellular and secreted HBsAg quantification in Huh7 transfectants with sWT or variant constructs via the Abbott luminescence platform. (b-c) Internal HBsAg detection in Huh7 transfectants with sWT or variants by non-reducing (b) and reducing (c) immunoblotting. (d-e) Cellular and secreted HA detection in Huh7 transfectants with sWT or variants via non-reducing (d) and reducing (e) immunoblotting. (f) Structural comparison and conformational variance of SHBs dimers between sWT and sC138R. Triplicate determinations; averages ± SD. $P < 0.001$

The C138R mutation reduced HBsAg secretion, antigenicity and immunogenicity in mice

For in vivo corroboration, HBV 1.3 and HBV C138R constructs were delivered to mice through rapid tail vein hydrodynamic administration **(Figure 6a).** In HBV 1.3 recipients, circulating HBsAg surged to maximum on day 3, then tapered to near-background by day 10. Anti-HBs titers emerged around day 7 and escalated through day 21. Conversely, HBV C138R animals displayed persistently negligible serum HBsAg throughout. Anti-HBs signals appeared solely on days 14 and 21, at markedly attenuated levels versus the HBV 1.3 cohort **(Figures 6b and d).** Liver HBsAg staining peaked on day 3 in HBV 1.3 mice before waning, while HBV C138R livers exhibited profoundly suppressed expression **(Figure 6c).** These animal data reinforced that the C138R variant severely hampers HBsAg export, epitope accessibility, and immune provocation.

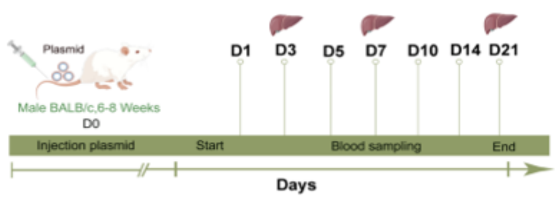

a)

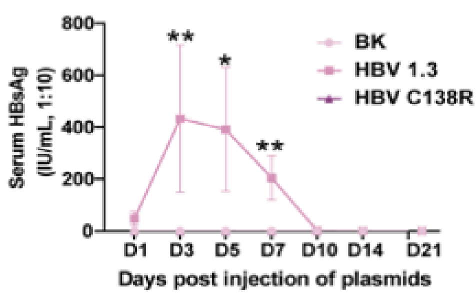

b)

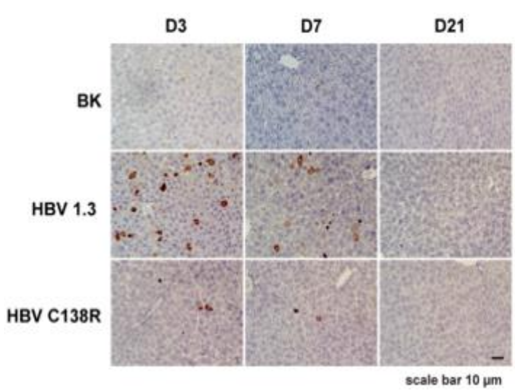

c)

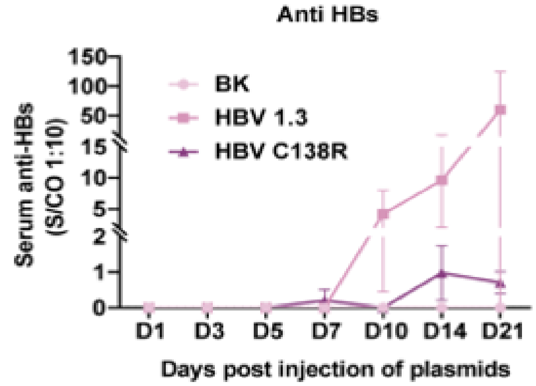

d)

Figure 6. The C138R variant suppressed HBsAg export, epitope exposure, and immune stimulation in the murine system. (a) Diagrammatic representation of the HBV murine model construction and timeline for specimen acquisition. (b) Circulating HBsAg concentrations determined by Abbott luminescence platform (n = 15 on days 1, 3; n = 10 on days 5, 7; n = 5 on days 10, 14, 21 per cohort). (c) Liver tissue HBsAg abundance was evaluated via immunohistochemical staining (n = 5 on days 3, 7, and 21 per cohort). (d) Circulating anti-HBs titers measured by Abbott luminescence platform (n = 15 on days 1, 3; n = 10 on days 5, 7; n = 5 on days 10, 14, 21 per cohort). Values expressed as average ± SD. P < 0.05, P < 0.01

The C138R alteration emerged from sequencing HBV S gene isolates derived from individuals exhibiting occult infection in our earlier investigations. Dating back to 2003, an analogous change was documented in patients with cirrhosis who had previously developed anti-HBs seroconversion [16]. Later reports substantiated its occurrence in occult cases [17, 18]. Nevertheless, the functional consequences of C138R on HBsAg properties and broader viral characteristics had not been elucidated. Here, complete HBV genomic constructs bearing the C138R change were introduced separately into three distinct cellular systems. Outcomes revealed profound depletion of HBsAg both within cells and in culture media, often approaching background detection thresholds. Importantly, the variant spared viral gene activation, genome amplification, production of alternative proteins, and even HBsAg transcript abundance. Such selectivity implied interference at post-transcriptional stages, potentially involving synthesis efficiency, protein folding, stability, or epitope accessibility. Positioned inside the ‘α’ determinant—a domain pivotal for immune recognition [21]—residue 138 prompted initial scrutiny of antigenic impacts. Accordingly, HA-fused wild-type (sWT) and variant (sC138R) vectors were engineered, leveraging the tag's neutrality toward HBsAg biogenesis and detection to accurately gauge protein output [22]. Assays disclosed marked intracellular HBsAg attenuation with the variant, contrasted by preserved or modestly elevated HA signals. Diagnostic ELISA panels exhibited variable but consistently diminished binding to the altered protein across manufacturers. Together, these observations established profound antigenic compromise by the solitary C138R substitution—a novel revelation, as prior work on alternative replacements at this locus (e.g., C138A, C138Y) typically incorporated tag-based monitoring from inception without isolating antigenic effects [19, 23].

Initial data attributed depleted HBsAg signals predominantly to recognition failure. Deeper analysis, however, uncovered an additional export deficiency accounting for extracellular scarcity. Robust HA signals appeared in media from wild-type transfectants yet vanished almost entirely from variant cultures, despite comparable or augmented internal HA accumulation. Corroborating ELISA metrics quantified sharply curtailed export ratios for the altered protein. Aligning with these results, earlier examinations of distinct substitutions at position 138 (e.g., C138A, triple C137/138/139A, C138Y) similarly documented secretory blockade [19, 23]. Thus, residue 138 emerges as essential for both immune visibility and trafficking. This report pioneers evidence that one isolated change at this site can concurrently undermine antigenic integrity and secretory competence.

The major hydrophilic region harbors multiple cysteines forming three conserved bridges: between residues 107-138, 124-137, and 139-147 [10]. Conventional models emphasize the ‘a’ determinant as a conformationally constrained loop anchored by the latter two pairings, deemed vital for structural fidelity and epitope presentation [10, 11]. Unexpectedly, our disruptions identified exclusive severity from abrogating the 107-138 linkage (via C107R or C138R), yielding dual antigenic and secretory deficits. The 124 bridge interruption mildly influenced recognition without compromising export, mirroring secreted HA equivalence to wild-type. Altering the 139-147 pairing exerted negligible influence on either parameter, aligning with luminescence and immunoblot equivalence to controls. As far back as 1995, solitary modification at 147 was shown inert toward these functions, challenging assignments of structural primacy to a 139-147 loop [19], a stance reinforced subsequently [23]. Consequently, the 107-138 linkage assumes paramount importance for ‘a’ determinant or broader MHR integrity, surpassing the other pairings in functional weight. Its rupture by C138R profoundly destabilizes conformation, driving the observed bipartite dysfunction in antigenicity and release.

Earlier research proposed the presence of SHBs dimers through computational modeling and site-directed mutagenesis studies [24-27]. Starting from 2022, multiple groups have verified SHBs dimer formation via cryo-electron microscopy combined with 3D reconstruction, indicating that such dimers constitute the core building blocks of spherical subviral particles (SVPs) [28-30]. In the present work, we initially applied a non-reducing Western blot (WB) approach to examine HBsAg, a technique that preserves disulfide linkages and thereby retains the natural dimeric or oligomeric states of the protein. Intracellular HBsAg from both the HBV 1.3 and sWT samples displayed a strong band near 40 kDa alongside a weak band around 20 kDa, suggesting that this assay predominantly identified SHBs dimers. In contrast, the C138R mutant sample revealed only a weak band close to 20 kDa, with the 40 kDa band barely visible. Notably, intracellular HA expressed from the sC138R construct showed a distinct band at approximately 40 kDa, with intensity similar to that observed in the sWT sample. These data indicated that the C138R substitution disrupted detection of SHBs dimers. To confirm this finding, we next conducted a reducing WB assay incorporating agents like DTT to break disulfide bonds, allowing visualization of linear epitopes on SHBs monomers. Under reducing conditions, both wild-type and C138R mutant samples exhibited strong HBsAg bands near 20 kDa, with comparable signal strengths between the two groups. This outcome implied that the C138R change specifically hindered detection of conformational epitopes in SHBs dimers while leaving linear monomeric epitopes unaffected. Such impairment likely stemmed from disruption of the disulfide linkage between residues 138 and 107, potentially allowing the newly exposed cysteine at position 107 to create improper intra- or inter-molecular bonds with other cysteines. These alterations could generate abnormally folded SHBs dimers that obscure key antigenic sites. Predictions generated by

AlphaFold 3 offered supportive evidence for these observations by highlighting clear structural distinctions between wild-type and C138R SHBs dimers. Nevertheless, these computational results remain preliminary and model-based only. Definitive confirmation will require experimental methods such as co-crystallization, chemical cross-linking coupled with mass spectrometry, or cryo-electron microscopy. Additionally, the results suggest that suitable pre-processing steps to disassemble spherical SVPs or dimers into monomers might unmask hidden epitopes, thus boosting HBsAg detection sensitivity and strengthening diagnostic performance in occult HBV infection (OBI).

Likewise, defective SHBs dimer folding may primarily account for the observed defect in HBsAg secretion. Beyond the C138R variant, prior reports have documented secretion defects with C138A and C138Y changes [19, 23], implying a shared pathway by which alterations at this position compromise HBsAg export. SHBs are mainly released as spherical SVPs through a process in which dimers form quickly in the endoplasmic reticulum (ER), are then bound by Sec24A, and are shuttled in COPII-coated vesicles to the ER-Golgi intermediate compartment (ERGIC) for multimerization into SVPs. Mature SVPs subsequently bud and move to the Golgi for maturation before extracellular release via exocytosis [27,31,32]. Misconfigured SHBs dimers may evade efficient Sec24A binding, preventing vesicular transport to the ERGIC and blocking SVP assembly. Alternatively, even if SVPs assemble, defective dimers might hinder proper budding or Golgi trafficking. These possibilities could underlie the consistent secretion blockade seen across different substitutions at residue 138.

In vivo experiments in mice reinforced these conclusions, demonstrating substantial reductions in HBsAg antigenicity, secretion, and immunogenicity following transfection with the HBV C138R construct. Here, the murine HBV model was created via hydrodynamic tail vein delivery, an effective and straightforward technique for assessing mutational impacts on HBsAg behavior in a living system. However, detectable HBsAg in liver and serum persisted for roughly 10 days only, failing to mimic the prolonged nature of chronic HBV infection. Upcoming investigations might employ lentiviral, adenoviral, or similar vectors to package the HBV genome and generate persistent infection models, enabling deeper evaluation of C138R effects on HBsAg in conditions resembling OBI more faithfully. Additional constraints of this work include its restriction to genotype B, the background in which C138R was first detected in an OBI case; broader testing across other HBV genotypes is needed to fully gauge the mutation's influence on HBsAg and viral traits. Moreover, diminished antigenicity and secretion due to C138R could promote intracellular HBsAg buildup. This retention, paired with lowered immunogenicity, might dampen immune surveillance and elimination of infected cells, favoring viral persistence [33, 34]. It could also induce ER stress and liver damage [35-37]. Additional research is required to clarify the host consequences of the C138R variant, especially its contribution to OBI onset and evolution.

Conclusion

Overall, our investigation showed that the C138R substitution concurrently compromised HBsAg antigenicity and secretion, playing a key role in OBI pathogenesis. We further established that loss of the disulfide bridge linking residues 107 and 138 drove formation of improperly configured dimers, serving as the chief cause of HBsAg malfunction in this mutant. Additionally, we verified the essential function of this bond in maintaining the structure of the 'a' determinant and major hydrophilic region (MHR). Together, these insights offer a mechanistic framework and fresh perspectives on OBI development and diagnostic strategies.

Acknowledgments: None

Conflict of Interest: None

Financial Support: None

Ethics Statement: None

References

1. Ponde RAA, Amorim GSP. Elimination of the hepatitis B virus: A goal, a challenge. Med Res Rev. 2024;44(5):2015–34.
2. Bucio-Ortiz L, Enriquez-Navarro K, Maldonado-Rodriguez A, et al. Occult hepatitis B virus infection in hepatic diseases and its significance for the WHO's elimination plan of viral hepatitis. Pathogens. 2024;13(8).
3. Raimondo G, Locarnini S, Pollicino T, et al. Update of the statements on biology and clinical impact of

occult hepatitis B virus infection. J Hepatol. 2019;71(2):397–408.
4. Seto WK, Chan TS, Hwang YY, et al. Hepatitis B reactivation in occult viral carriers undergoing hematopoietic stem cell transplantation: A prospective study. Hepatology. 2017;65(5):1451–61.
5. Shi Y, Wu YH, Wu W, et al. Association between occult hepatitis B infection and the risk of hepatocellular carcinoma: a meta-analysis. Liver Int. 2012;32(2):231–40.
6. Fu MX, Elsharkawy A, Healy B, et al. Occult hepatitis B virus infection: risk for a blood supply, but how about individuals' health? EClinicalMedicine. 2025;81:103095.
7. Chazouilleres O, Mamish D, Kim M, et al. Occult hepatitis B virus as source of infection in liver transplant recipients. Lancet. 1994;343(8890):142–6.
8. Zhang ZH, Wu CC, Chen XW, et al. Genetic variation of hepatitis B virus and its significance for pathogenesis. World J Gastroenterol. 2016;22(1):126–44.
9. Hao B, Liu Y, Wang B, et al. Hepatitis B surface antigen: carcinogenesis mechanisms and clinical implications in hepatocellular carcinoma. Exp Hematol Oncol. 2025;14(1):44.
10. Jiang X, Chang L, Yan Y, et al. Paradoxical HBsAg and anti-HBs coexistence among chronic HBV infections: causes and consequences. Int J Biol Sci. 2021;17(4):1125–37.
11. Zhu HL, Li X, Li J, et al. Genetic variation of occult hepatitis B virus infection. World J Gastroenterol. 2016;22(13):3531–46.
12. Wu C, Deng W, Deng L, et al. Amino acid substitutions at positions 122 and 145 of hepatitis B virus surface antigen (HBsAg) determine the antigenicity and immunogenicity of HBsAg and influence in vivo HBsAg clearance. J Virol. 2012;86(8):4658–69.
13. Xiang KH, Michailidis E, Ding H, et al. Effects of amino acid substitutions in hepatitis B virus surface protein on virion secretion, antigenicity, HBsAg and viral DNA. J Hepatol. 2017;66(2):288–96.
14. Huang CH, Yuan Q, Chen PJ, et al. Influence of mutations in hepatitis B virus surface protein on viral antigenicity and phenotype in occult HBV strains from blood donors. J Hepatol. 2012;57(4):720–9.
15. Kalinina T, Iwanski A, Will H, et al. Deficiency in virion secretion and decreased stability of the hepatitis B virus immune escape mutant G145R. Hepatology. 2003;38(5):1274–81.
16. Mathet VL, Feld M, Espinola L, et al. Hepatitis B virus S gene mutants in a patient with chronic active hepatitis with Circulating Anti-HBs antibodies. J Med Virol. 2003;69(1):18–26.
17. He C, Liu Y, Jiang X, et al. Frequency of HBsAg variants in occult hepatitis B virus infected patients and detection by ARCHITECT HBsAg quantitative. Front Cell Infect Microbiol. 2024;14:1368473.
18. Enriquez-Navarro K, Maldonado-Rodriguez A, Rojas-Montes O, et al. Identification of mutations in the S gene of hepatitis B virus in HIV positive Mexican patients with occult hepatitis B virus infection. Ann Hepatol. 2020;19(5):507–15.
19. Mangold CM, Unckell F, Werr M, et al. Secretion and antigenicity of hepatitis B virus small envelope proteins lacking cysteines in the major antigenic region. Virology. 1995;211(2):535–43.
20. Zhang Z, Trippler M, Real CI, et al. Hepatitis B virus particles activate Toll-Like receptor 2 signaling initially upon infection of primary human hepatocytes. Hepatology. 2020;72(3):829–44.
21. Wu CC, Chen YS, Cao L, et al. Hepatitis B virus infection: defective surface antigen expression and pathogenesis. World J Gastroenterol. 2018;24(31):3488–99.
22. Powell EA, Boyce CL, Gededzha MP, et al. Functional analysis of 'a' determinant mutations associated with occult HBV in HIV-positive South Africans. J Gen Virol. 2016;97(7):1615–24.
23. Kwei K, Tang X, Lok AS, et al. Impaired virion secretion by hepatitis B virus immune escape mutants and its rescue by wild-type envelope proteins or a second-site mutation. J Virol. 2013;87(4):2352–7.
24. Gilbert RJ, Beales L, Blond D, et al. Hepatitis B small surface antigen particles are octahedral. Proc Natl Acad Sci U S A. 2005;102(41):14783–8.
25. Suffner S, Gerstenberg N, Patra M, et al. Domains of the hepatitis B virus small surface protein S mediating oligomerization. J Virol. 2018;92(11).
26. Wounderlich G, Bruss V. Characterization of early hepatitis B virus surface protein oligomers. Arch Virol. 1996;141(7):1191–205.
27. Yang S, Shen Z, Kang Y, et al. A putative amphipathic alpha helix in hepatitis B virus small

envelope protein plays a critical role in the morphogenesis of subviral particles. J Virol. 2021;95(8).

28. Liu H, Hong X, Xi J, et al. Cryo-EM structures of human hepatitis B and woodchuck hepatitis virus small spherical subviral particles. Sci Adv. 2022;8(31):eabo4184.
29. Wang Q, Wang T, Cao L, et al. Inherent symmetry and flexibility in hepatitis B virus subviral particles. Science. 2024;385(6714):1217–24.
30. He X, Kang Y, Tao W, et al. Structure of small HBV surface antigen reveals mechanism of dimer formation. Cell Discov. 2025;11(1):6.
31. Huovila AP, Eder AM, Fuller SD. Hepatitis B surface antigen assembles in a post-ER, pre-Golgi compartment. J Cell Biol. 1992;118(6):1305–20.
32. Zeyen L, Doring T, Stieler JT, et al. Hepatitis B subviral envelope particles use the COPII machinery for intracellular transport via selective exploitation of Sec24A and Sec23B. Cell Microbiol. 2020;22(6):e13181.
33. Jiang M, Broering R, Trippler M, et al. Toll-like receptor-mediated immune responses are attenuated in the presence of high levels of hepatitis B virus surface antigen. J Viral Hepat. 2014;21(12):860–72.
34. Qi R, Fu R, Lei X, et al. Therapeutic vaccine-induced plasma cell differentiation is defective in the presence of persistently high HBsAg levels. J Hepatol. 2024;80(5):714–29.
35. Liang Y, Luo X, Schefczyk S, et al. Hepatitis B surface antigen expression impairs Endoplasmic reticulum stress-related autophagic flux by decreasing LAMP2. JHEP Rep. 2024;6(4):101012.
36. Peiffer KH, Akhras S, Himmelsbach K, et al. Intracellular accumulation of subviral HBsAg particles and diminished Nrf2 activation in HBV genotype G expressing cells lead to an increased ROI level. J Hepatol. 2015;62(4):791–8.
37. Pollicino T, Cacciola I, Saffioti F, et al. Hepatitis B virus PreS/S gene variants: pathobiology and clinical implications. J Hepatol. 2014;61(2):408–17.